molecular pharmaceutics

communications

Mechanistic Examination of Protein Release from Polymer Nanofibers

M. Gandhi,[†] R. Srikar,[‡] A. L. Yarin,[‡] C. M. Megaridis,[‡] and R. A. Gemeinhart*[,†,§]

Department of Biopharmaceutical Sciences, University of Illinois, Chicago, Illinois 60612-7231, Department of Mechanical and Industrial Engineering, University of Illinois, Chicago, Illinois 60607-7022, and Department of Bioengineering, University of Illinois, Chicago, Illinois 60607-7052

Received September 9, 2008
Revised Manuscript Received January 16, 2009
Accepted January 24, 2009

Abstract: Therapeutic proteins have emerged as a significant class of pharmaceutical agents over the past several decades. The potency, rapid elimination, and systemic side effects have prompted the need of spatiotemporally controlled release for proteins maybe more than any other active therapeutic molecules. This work examines the release of two model protein compounds, bovine serum albumin (BSA) and an anti-integrin antibody (AI), from electrospun polycaprolactone (PCL) nanofiber mats. The anti-integrin antibody was chosen as a model of antibody therapy; in particular, anti-integrin antibodies are a promising class of therapeutic molecules for cancer and angiogenic diseases. The release kinetics were studied experimentally and interpreted in the framework of a recently published theory of desorption-limited drug release from nondegrading—or very slowly degrading—fibers. The results are consistent with a protein release mechanism dominated by desorption from the polymer surface, while the polycaprolactone nanofibers are not degrading at an appreciable rate.

Keywords: Nanofiber; protein; modeling; controlled release

Proteins have been growing as a class of therapeutic molecules over the past several decades.[1] Although much progress on oral protein delivery has been made,[2] most protein therapeutics must be delivered by parenteral, i.e. not oral, routes of administration. Typical injections, e.g. subcutaneous, intravenous, or intramuscular, allow proteins to act in a systemic manner before the proteins rapidly degrade and are eliminated from the body. To overcome these issues associated with proteins, local protein release from polymeric carriers has been utilized.[3] Protein release from polymeric structures has been modeled[4] and used to improve the design of drug delivery systems.[5−7] Even though the majority of clinically applied systems have not varied greatly from the original designs of controlled release systems,[3,8] recent advances in protein modification[9] can be used in combination with polymeric materials[10] to alter the distribution of the therapeutic molecules around the device. However, such procedures involve modification of the protein, which creates significant regulatory challenges. As an alternative, methods that better control the release of therapeutic proteins are needed. One alternative to modifying active proteins is to develop novel polymer structures containing proteins and understand the fundamental release mechanisms from these structures.

As novel polymeric structures, electrospun polymer fibers can be easily and reproducibly made[11] with small-molecule drug[12] or protein molecules[13] encapsulated within the fibers for eventual release. Nanofibers are routinely produced by electrospinning,[14] a process operated at room temperature,

* To whom correspondence should be addressed. Mailing address: 833 S. Wood St., Chicago, IL 60612-7231. E-mail: rag@uic.edu. Tel: +1(312) 996-2253. Fax: +1(312) 996-2784.
[†] Department of Biopharmaceutical Sciences.
[‡] Department of Mechanical and Industrial Engineering.
[§] Department of Bioengineering.

(1) Spada, S.; Walsh, G. *Directory of Approved Biopharmaceutical Products*; CRC Press: Boca Raton, FL, 2005.
(2) Gemeinhart, R. A. Polymeric Systems for Oral Protein and Peptide Delivery. In *Pharmaceutical Biotechnology*, 2nd ed.; Groves, M. J., Ed.; Taylor & Francis CRC Press: Boca Raton, FL, 2005; pp *279*−302.
(3) Langer, R.; Folkman, J. Polymers for the Sustained Release of Proteins and Other Macromolecules. *Nature* **1976**, *263* (5580), 797–800.
(4) Saltzman, W. M.; Langer, R. Transport Rates of Proteins in Porous Materials with Known Microgeometry. *Biophys. J.* **1989**, *55* (1), 163–71.
(5) Mahoney, M. J.; Saltzman, W. M. Controlled Release of Proteins to Tissue Transplants for the Treatment of Neurodegenerative Disorders. *J. Pharm. Sci.* **1996**, *85* (12), 1276–81.
(6) Weinberg, B. D.; Patel, R. B.; Exner, A. A.; Saidel, G. A.; Gao, J. M. Modeling Doxorubicin Transport to Improve Intratumoral Drug Delivery to Rf Ablated Tumors. *J. Controlled Release* **2007**, *124* (1−2), 11–9.
(7) Wang, F. J.; Saidel, G. M.; Gao, J. M. A Mechanistic Model of Controlled Drug Release from Polymer Millirods: Effects of Excipients and Complex Binding. *J. Controlled Release* **2007**, *119* (1), 111–20.
(8) Folkman, J.; Long, D. M. The Use of Silicone Rubber as a Carrier for Prolonged Drug Therapy. *J. Surg. Res.* **1964**, *71*, 139–42.
(9) Pasut, G.; Sergi, M.; Veronese, F. M. Anti-Cancer Peg-Enzymes: 30 years Old, but Still a Current Approach. *Adv. Drug Delivery Rev.* **2008**, *60* (1), 69–78.

10.1021/mp800160p CCC: $40.75
Published on Web 01/24/2009

with electrical fields and mechanical stresses that are not harmful to biologically active substances.[15,16] Such substances can be blended relatively easily in polymer solutions and then electrospun using standard electrospinning setups. Several low molecular weight compounds, including model fluorescent dyes[12] and drugs,[17] as well as high molecular weight proteins, growth factors and protein-based drugs,[18−22] have been electrospun and released from nanofibers. Related procedures also allow live organisms, including active viruses, to be electrospun and embedded in nanofibers.[16,23]

Even though the release kinetics were studied experimentally for a number of substances, the physicochemical mechanisms of drug release have not been fully elucidated. Recent work argued that, under specific conditions, the release mechanism is governed by desorption, or dissolution, from nanopores on the surface rather than by a solid state diffusion mechanism.[12] Satisfactory agreement between the desorption-limited mechanism and the experimental data of the release kinetics for a low molecular weight ($M_w = 479.02$ Da) model compound, specifically fluorescent dye rhodamine 610 chloride, from polymer nanofibers was demonstrated.[12] In the present work, the release kinetics of bovine serum albumin (BSA) and anti-$\alpha_v\beta_3$ integrin IgG antibody (AI) are examined as representative proteins. Various vaccines and protein pharmaceuticals contain BSA or human albumin as a stabilizing agent or excipient.[24,25] In the present case, BSA was investigated both as a model protein, as well as an excipient for the addition of other higher potency proteins, specifically AI.

Antibodies to the $\alpha_v\beta_3$ integrin have been investigated for antiangiogenic potential and were thus utilized as a model for local antibody therapy.[26] This compound was chosen for the therapeutic potential against cancer and angiogenesis-based diseases, including macular degeneration.[26] AI binds to $\alpha_v\beta_3$ integrins that are known to be expressed on neovascular tissues[27] and thus inhibit vascular growth. At least three antibody therapies are in clinical trials at this time.[26] Specifically, AI prevents the attachment of endothelial cells to ECM during the tube formation phase of angiogenesis, thus acting as an antiangiogenesis agent and one of the promising candidates for cancer therapy. The aim of the experiment of the present work with AI was to evaluate its release in the presence of BSA. The release of these two model proteins were in good agreement with theory considering that desorption from the surface of the nanofiber did, in fact, predominate as a delivery mechanism prior to appreciable degredation.

Albumin (BSA) is the predominant serum protein with molecular weight of 66 kDa from the bovine source used. Alexa Fluor 488 conjugated BSA (Invitrogen, Catalog No. A13100) was used in the experiments to facilitate quantitative assessment of release. Nanofibers were electrospun from polycaprolactone (PCL). Polycaprolactone ($M_w = 80$ kDa) was dissolved in 60:40 (w/w) ratio of dimethylformamide (DMF) and methylene chloride (MC). PCL, DMF and MC were supplied by Sigma-Aldrich and used as received. Following previously published methods, three concentrations of PCL, namely, 11%, 13% and 15% (w/w) in DMF/

(10) Haverstick, K.; Fleming, A.; Saltzman, W. M. Conjugation to Increase Treatment Volume During Local Therapy: A Case Study with Pegylated Camptothecin. *Bioconjugate Chem.* **2007**, *18* (6), 2115–21.
(11) Reneker, D. H.; Yarin, A. L.; Zussman, E.; Xu, H. Electrospinning of Nanofibers from Polymer Solutions and Melts. *Adv. Appl. Mech.* **2007**, *41*, 43–195.
(12) Srikar, R.; Yarin, A. L.; Megaridis, C. M.; Bazilevsky, A. V.; Kelley, E. Desorption-Limited Mechanism of Release from Polymer Nanofibers. *Langmuir* **2008**, *24* (3), 965–74.
(13) Maretschek, S.; Greiner, A.; Kissel, T. Electrospun Biodegradable Nanofiber Nonwovens for Controlled Release of Proteins. *J. Controlled Release* **2008**, *127* (2), 180–7.
(14) Greiner, A.; Wendorff, J. H.; Yarin, A. L.; Zussman, E. Biohybrid Nanosystems with Polymer Nanofibers and Nanotubes. *Appl. Microbiol. Biotechnol.* **2006**, *71* (4), 387–93.
(15) Reznik, S. N.; Yarin, A. L.; Zussman, E.; Bercovici, L. Evolution of a Compound Droplet Attached to a Core-Shell Nozzle under the Action of a Strong Electric Field. *Phys. Fluids* **2006**, *18* (6), 062101-1–062101-13.
(16) Salalha, W.; Kuhn, J.; Dror, Y.; Zussman, E. Encapsulation of Bacteria and Viruses in Electrospun Nanofibres. *Nanotechnology* **2006**, *17* (18), 4675–81.
(17) Kenawy, E. R.; Bowlin, G. L.; Mansfield, K.; Layman, J.; Simpson, D. G.; Sanders, E. H.; Wnek, G. E. Release of Tetracycline Hydrochloride from Electrospun Poly(Ethylene-Co-Vinylacetate), Poly(Lactic Acid), and a Blend. *J. Controlled Release* **2002**, *81* (1−2), 57–64.
(18) Chew, S. Y.; Wen, J.; Yim, E. K. F.; Leong, K. W. Sustained Release of Proteins from Electrospun Biodegradable Fibers. *Biomacromolecules* **2005**, *6* (4), 2017–24.
(19) Kowalczyk, T.; Nowicka, A.; Elbaum, D.; Kowalewski, T. A. Electrospinning of Bovine Serum Albumin. Optimization and the Use for Production of Biosensors. *Biomacromolecules* **2008**, *9* (7), 2087–90.
(20) Li, C. M.; Vepari, C.; Jin, H. J.; Kim, H. J.; Kaplan, D. L. Electrospun Silk-Bmp-2 Scaffolds for Bone Tissue Engineering. *Biomaterials* **2006**, *27* (16), 3115–24.
(21) Moroni, L.; Licht, R.; de Boer, J.; de Wijn, J. R.; van Blitterswijk, C. A. Fiber Diameter and Texture of Electrospun Peot/Pbt Scaffolds Influence Human Mesenchymal Stem Cell Proliferation and Morphology, and the Release of Incorporated Compounds. *Biomaterials* **2006**, *27* (28), 4911–22.
(22) Zong, X. H.; Kim, K.; Fang, D. F.; Ran, S. F.; Hsiao, B. S.; Chu, B. Structure and Process Relationship of Electrospun Bioabsorbable Nanofiber Membranes. *Polymer* **2002**, *43* (16), 4403–12.
(23) Lee, S. W.; Belcher, A. M. Virus-Based Fabrication of Micro- and Nanofibers Using Electrospinning. *Nano Lett.* **2004**, *4* (3), 387–90.
(24) Saha, P.; Kou, J. H. Effect of Bovine Serum Albumin on Drug Permeability Estimation across Caco-2 Monolayers. *Eur. J. Pharm. Biopharm.* **2002**, *54* (3), 319–24.
(25) Sánchez, A.; Villamayor, B.; Guo, Y.; McIver, J.; Alonso, M. J. Formulation Strategies for the Stabilization of Tetanus Toxoid in Poly(Lactide-Co-Glycolide) Microspheres. *Int. J. Pharm.* **1999**, *185* (2), 255–66.
(26) Avraamides, C. J.; Garmy-Susini, B.; Varner, J. A. Integrins in Angiogenesis and Lymphangiogenesis. *Nat. Rev. Cancer* **2008**, *8* (8), 604–17.
(27) Arap, W.; Pasqualini, R.; Ruoslahti, E. Cancer Treatment by Targeted Drug Delivery to Tumor Vasculature in a Mouse Model. *Science* **1998**, *279* (5349), 377–80.

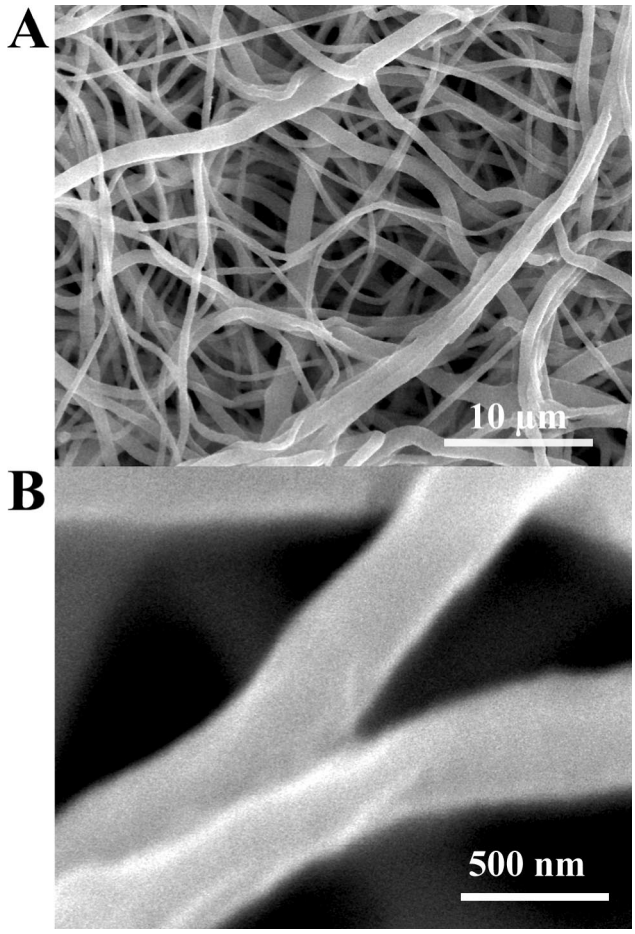

Figure 1. Scanning electron micrographs of electrospun polycaprolactone nanofiber mat (A, scale bar 10 μm) and individual nanofibers (B, scale bar 500 nm) containing bovine serum albumin.

MC, were evaluated for BSA release.[12] BSA (50 μg of BSA/g of PCL) was dissolved in the DMF/MC solution.

The electrospinning parameters employed for generating nanofibers included a flow rate of 1 mL/h for all polymer concentrations, a voltage of 12.5 kV for 11%, 13.5 kV for 13% and 15% PCL solutions, and an interelectrode distance of 14 cm for 11% and 13%, and 12 cm for 15% PCL solutions. The electrospun nonwoven PCL nanofiber mats containing BSA were collected on a planar, grounded, disk-shaped metal electrode. The nanofibers in these mats had average cross-sectional diameters in the range 500 to 700 nm based on previously reported results where scanning electron microscopy (SEM) observations were made.[12] Similar diameter nanofibers were observed (Figure 1).

The as-spun nanofiber mats were cut into sections using a scalpel and weighed on a microbalance to evaluate the theoretical loaded protein mass from the known mass ratio of PCL to protein assuming that there was no loss of protein or PCL and that all solvent had evaporated. Three samples of PCL nanofiber sections (83 $\pm$ 0.3 mg) were placed in compartments of a 24-well plate each with 1 mL of phosphate buffer saline, PBS. This amounted to 4.15 $\pm$ 0.1 μg of BSA per sample. The microwell plates were kept on a mechanical shaker at room temperature during release. BSA release was measured (Gemini Spectramax spectrofluorometer; Molecular Devices) in PBS using a calibration curve established in preliminary experiments with known concentrations of BSA in PBS in the range of 0.5 to 200 μg/mL BSA (R^2 = 0.991). At predetermined time periods, the medium was removed and 100 μL samples were measured at excitation and emission wavelengths of 497 and 520 nm, respectively. The remainder of the PBS in the sample was removed and fresh 1 mL of PBS was added. A minimum of three independent replicates were examined.

In another set of experiments, anti-$\alpha_v\beta_3$ integrin IgG antibody (M_w = 116.038 kDa), AI, was used as a model therapeutic protein. Mouse antihuman integrin $\alpha_v\beta_3$ IgG1 monoclonal antibody conjugated with r-phycoerythrin (Chemicon International, Catalog No. MAB1976H) and BSA were used in the experiment of AI release. Similar to the previously described experiment with BSA, an 11% PCL solution was prepared in 60:40 (w:w) DMF/MC solvent mixture. BSA was used as a diluent to investigate its effect on AI release. Three sets of experiments were carried out with constant AI loading (20 μg per gram of PCL) and BSA added in various weight ratios with respect to AI (AI:BSA ratios of 1:0, 1:1, 1:10 and 1:100). The electrospinning parameters were set at a flow rate of 1 mL/h, voltage of 12.5 kV, and an interelectrode distance of 14 cm. Sections of nonwoven mats were prepared similarly to the pure BSA case described previously. Fluorescence of these samples was measured at excitation and emission wavelengths of 488 and 580 nm, respectively, for AI and correlated with a standard curve. All measurements were replicated in triplicate independent samples. Both AI and BSA are fluorescent materials with similar excitation wavelengths. However, BSA and AI have very distinct emission peaks, which allowed accurate evaluation of AI content in the samples containing both AI and BSA. This was confirmed by measuring the fluorescence spectrum of PBS solutions containing both proteins. Also, we attempted to measure BSA concentration at the emission wavelength of AI (580 nm) but were unable to record any significant peak. The latter confimed that fluorescence measured at excitation and emission wavelengths of 488 and 580 nm, respectively, entirely represent AI concentration alone.

In order to examine the binding capacity of AI released from nanofiber mats, the binding of AI to cells known to express the $\alpha_v\beta_3$ integrin was examined. Human umbilical vein endothelial cells (HUVEC) were maintained in culture on tissue culture plastic using endothelial growth medium (EGM) supplemented with EGM-2 BulletKit (Lonza Group, Ltd.). The HUVECs (10^5 cells/mL) were plated on 24-well plates and incubated overnight. Transwell inserts were placed in the plates and nanofiber samples were placed in the upper chamber. As control groups, cells were incubated with AI (30 μg/mL) for one hour prior to the exposure to the nanofibers to confirm that antibody-cell interactions could be blocked and were specific. At various times after incubation, the morphology and presence of AI was docu-

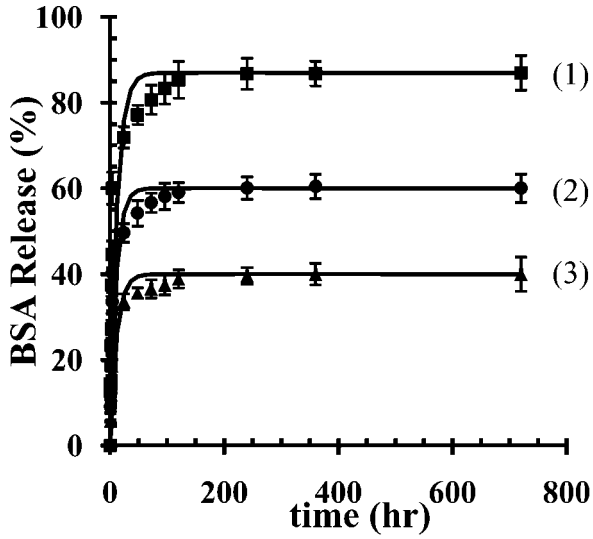

Figure 2. Effect of initial polymer concentration on BSA release from PCL nanofiber mats. The experimental data ($n = 3$; average ± SD) are shown by symbols, the corresponding theoretical prediction by the solid lines. The amount of BSA released in 30 days was 87% from 11% PCL (1-■), 60% from 13% PCL (2-●), and 40% from 15% PCL (3-▲).

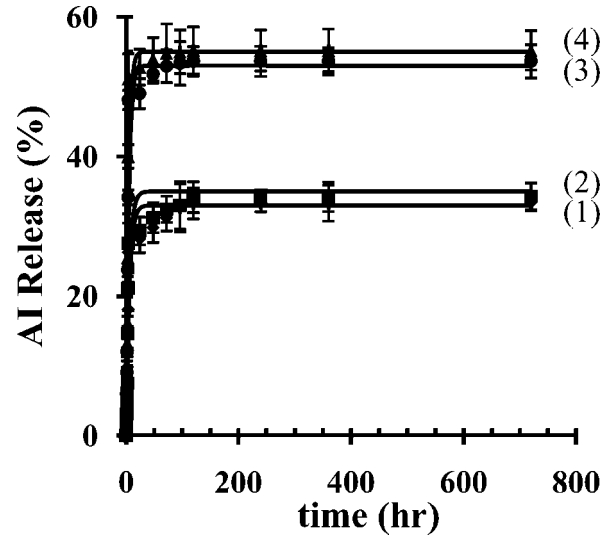

Figure 3. Effect of initial bovine serum albumin (BSA) content on anti-integrin IgG antibody (AI) release from 11% PCL nanofibers. The experimental data ($n = 3$; average ± SD) are shown by symbols, and the corresponding theoretical prediction by solid lines. When the initial AI mass was constant, (1-★) a 1:0 AI:BSA ratio resulted in 33% AI release at saturation, (2-■) a 1:1 AI:BSA ratio resulted in 35% AI release at saturation, (3-●) a 1:10 AI:BSA ratio resulted in 53% AI release at saturation, and (4-▲) a 1:100 AI:BSA ratio resulted in 55% of AI release at saturation within the 30 day period examined.

mented using an inverted phase-contrast, epifluorescence microscope (Olympus IX70) and digital images captured (QImaging Retiga 1300 C) and processed using available software (Scanalytics IP Laboratory).

Statistical significance was determined by analysis of variance (ANOVA) and Tukey posthoc test at the significance level of less than 0.05 ($p < 0.05$) using SPSS 14 software. Data points in the figures are presented as the mean plus or minus the standard deviation obtained from three independent samples.

BSA release (Figure 2) was significantly affected ($p < 0.01$) by the initial concentration of PCL in the feed solution. The release approached 87% in 30 days for 11% PCL with 60% released in the first 4 h. The samples with initial PCL content of 13% and 15% had lower BSA release levels at saturation, specifically 60% released in 30 days by 13% PCL fibers (40% in the first 4 h) and 40% released in 30 days by 15% PCL fibers (30% in the first 4 h).

The amount of AI released at saturation (between approximately 120 and 720 h) increased with the relative amount of BSA loaded in the nanofibers with respect to AI (Figure 3). In particular, the 1:0 AI:BSA ratio (no BSA present) had the lowest release at saturation compared to the cases where BSA was present. Specifically, PCL nanofibers having 1:0 AI:BSA ratio showed 33% AI release in 5 days, rather close ($p > 0.05$) to the 1:1 AI:BSA ratio case, which showed 35% AI release in 5 days (with approximately 27% released in the first 4 h in both cases). Released levels of AI from the nanofibers having the 1:10 and 1:100 AI:BSA ratios were significantly higher ($p < 0.01$). The 1:10 ratio nanofibers released 53% AI in 5 days (48% release in the first 4 h). The PCL fibers with the 1:100 AI:BSA ratio released 55% of loaded AI in 5 days (51% release in the first 4 h). This demonstrated that the release of a protein (in the present case, AI) from polymer nanofibers can be controlled by adding BSA in the formulation. The higher the amount of BSA added to the nanofibers, the higher the release of AI, even though the effect of BSA appears to saturate at about 1:10 AI:BSA ratio, possibly because at this ratio a maximal amount of BSA is available at the surface of the nanopores where desorption takes place. Based on theoretical estimates (see below), it is argued that desorption of BSA macromolecules from the PCL matrix facilitates desorption of AI significantly up to AI:BSA ratios of 1:10.

Additional biological experiments confirmed that released AI was able to bind to integrin expressing HUVEC cells (Figure 4). Nanofiber mats containing both AI and BSA (1:0, 1:1, 1:10 and 1:100 AI:BSA ratios) were placed in Transwell inserts to allow the effect of the nanofibers on cells to be neglected in the analysis. AI released was able to bind to the HUVECs and a qualitatively greater amount of fluorescence was observed in the groups (1:10 and 1:100 AI:BSA ratios) that released a greater amount of AI in the first day (compare with Figure 3). The cells which were blocked with antibodies (AI control) did not show any fluorescence confirming that released AI is specifically binding to the integrin expressed by HUVECs. This indicates that the electrospinning process did not completely denature the antibodies which were entrapped in the nanofibers. Denatured protein would be expected to bind to the cells

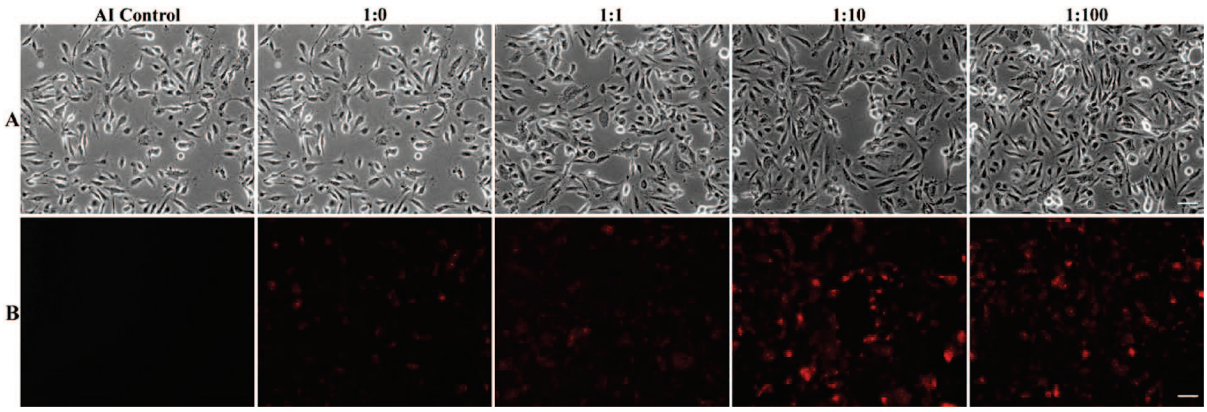

Figure 4. Binding of anti-integrin IgG antibody (AI) released from the nanofiber mats loaded with varying AI: BSA ratios (1:0, 1:1, 1:10 and 1:100 AI:BSA ratios) to integrin expressing human umbilical vein endothelial cells (HUVEC). Cells which were preblocked with anti-integrin $\alpha_v\beta_3$ antibodies (AI Control) without fluorescent tag did not show any fluorescence. Only the 1:10 AI:BSA ratio is shown as AI blocked control, but all groups exhibited no binding. (A) Light micrographs (scale bar 100 μm) show similar cell density and morphology while (B) epifluorescence imaging (scale bar 100 μm) showed higher AI binding in nanofiber groups that had greater protein release (1:10 and 1:100 AI:BSA ratios).

regardless of whether any specific sites were available or not. The fact that some denaturation occurred cannot be overlooked, and further experiments are needed to confirm the amount of denaturation that does take place in the process, if any.

This is exemplified by the fact that pure BSA nanofibers have been electrospun using a procedure which was designed to denature (unfold) BSA to increase its spinnability.[28] This suggests that proteins can easily be denatured by the electrospinning process under the wrong (or right in the case of the pure BSA nanofibers) conditions. In the present work, spinnability was provided by the host polymer, PCL with no need for BSA (or AI) denaturation. The conditions were controlled to limit the protein denaturation, but further optimization may be beneficial.

The desorption-limited theory of admixture release[12] from the nanofibrous material predicts the mass, G, released at any time, t (eq 1). In this, the nanoporosity factor (eq 2), α, is defined by the initial amount of protein admixture on the nanofiber surface, M_{sd0}, and the initial amount of the protein admixture embedded in the fiber bulk, M_{bd0}. The total initial amount of the protein admixture, M_{d0}, in the nanofibers is the sum of the surface protein admixture and embedded protein admixture (eq 3).

$$\frac{G}{M_{d0}} = \alpha\left[1 - \exp\left(-\frac{\pi^2}{8}\frac{t}{\tau_r}\right)\right] \quad (1)$$

$$\alpha = \frac{M_{sd0}}{M_{d0}} \quad (2)$$

$$M_{d0} = M_{sd0} + M_{bd0} \quad (3)$$

According to eq 1, the release process will saturate at a specific percent release at infinite time. For nanofibers fabricated from nondegrading materials, this would be the final released amount; however, for nanofibers fabricated out of degrading materials, another phase of release would be observed (and potentially modeled) due to degradation of the nanofibers. The saturation is dictated by the nanoporosity factor, α, which is related to the nanopore surface area and thus should depend on polymer concentration in the electrospun solution. This was demonstrated for low molecular weight compound (fluorescent dye) release from 11−15% PCL nanofiber mats.[12] The results of the present work with proteins (Figure 2) demonstrate the same trend: the lower the initial PCL concentration, the more porous the resulting nanofibers are, which facilitates higher saturated percent BSA release. On the contrary, the characteristic time, τ_r, in eq 1 is related (eq 4) to the nanopore length, L, and effective diffusion coefficient, D_{eff}. The effective diffusion coefficient depends (eq 5) on the kinetic parameters, k_0 and E, of the desorption process [the pre-exponential, k_0, and desorption enthalpy or activation energy, E, respectively], the protein diffusion coefficient in PBS, D, the nanopore cross-sectional radius, b, the gas constant, R, the temperature, T, and the surface density of PCL, ρ_{sp}. The characteristic time determines the time scale of the release process (a significant variation of the released mass G is felt only at t of the order of τ_r; cf. ref 12). The pre-exponential, k_0, and desorption enthalpy, E, characterize the intermolecular forces binding the admixture molecules and the polymer surface in the presence of release media, i.e. PBS. Therefore, τ_r, k_0 and E are expected to be insensitive to the polymer (PCL) concentration. These quantities should manifest only the chemical nature of the PCL−admixture interactions responsible for sorption−desorption processes in the presence of water or PBS. In the case of simultaneous release of two admixture compounds (AI and BSA,

(28) Dror, Y.; Ziv, T.; Makarov, V.; Wolf, H.; Admon, A.; Zussman, E. Nanofibers Made of Globular Proteins. *Biomacromolecules* **2008**, *9* (10), 2749–54.

for example), these parameters should be sensitive to the amount of AI present, as compared to the release of pure BSA.

$$\tau_r = \frac{L^2}{D_{eff}} \quad (4)$$

$$D_{eff} = \frac{Dbk_0}{\rho_{sp}} \exp\left(-\frac{E}{RT}\right) \quad (5)$$

It is emphasized that, at the beginning of the release process, at times shorter that the characteristic time τ_r, eq 1 reduces to linear dependence of G on t (via Taylor series expansion; eq 6). The seemingly bilinear release behavior in Figures 2 and 3, namely, an almost linear initial increase of the released mass, followed by an almost saturated plateau at longer times as the characteristic time is approached. Both seemingly linear regions are, therefore, related to the desorption-limited mechanism of release[12] and are in agreement with the general nonlinear theory (eq 1).

$$\frac{G}{M_{d0}} = \alpha\frac{\pi^2}{8}\frac{t}{\tau_r} \quad (6)$$

If the geometric and molecular parameters of the desorption process are all known in detail, the corresponding value of τ_r can be calculated independently. Typically, only their orders of magnitude are available, which allows only order of magnitude estimation.[12] As usual in such cases, utilizing eq 1 with the experimental data in Figures 2 and 3 allows one to establish the parameters of the desorption characteristics of BSA and AI:BSA release (Table 1).

The curves generated from fitting eq 1 closely fit the data with an appropriate choice of τ_r and α. Once the value of τ_r is established, the value of an effective diffusion coefficient, D_{eff}, can be calculated. As an order of magnitude estimate, the value of the characteristic nanopore length, L, was taken as 1000 nm, which is quite reasonable for nanofibers with average cross-sectional diameters on the order of 700 nm. The fact that the fit is order of magnitude is one reason that the fit curves do not precisely match data. The values of τ_r and D_{eff} obtained with this estimation are presented (Table 1). The desorption factor, $k(T)$, is described by the Clapeyron-like (or the Arrhenius-like) dependence (eq 7) with the pre-exponential, k_0, having dimensionality of density (g/cm^3). The values of τ_r and D_{eff} appear to be essentially insensitive to PCL concentration, similar to the previous findings for small-molecule dye release from 11−15% PCL nanofibers. The values of the desorption enthalpy, E, are only slightly higher than the values of E = 37.3−37.8 kJ/mol found for release of low molecular weight fluorescent dye.[12] The increase of E to the level of 38.2−39.3 kJ/mol constitutes the effect of a change in the chemical nature of the released compound, as well as of an increase in its molecular weight. Although this does suggest that the desorption energy is influenced by the chemistry of the released molecule, the specific interactions are not accounted for in this theory. Overall, desorption of the fluorescent dye, rhodamine 610 chloride, from PCL nanofibers is more favored than that of BSA. However, presence and release of high molecular weight BSA macromolecules seemingly promote development of nanoporosity, which, for example, results in the higher values of the nanoporosity coefficient α for BSA (0.4−0.87) than the corresponding values of α = 0.32−0.67 for rhodamine 610 chloride.[12]

Table 1. Basic Release Parameters Including the Desorption Enthalpy, E, and Nanoporosity Factor, α, for Polymer Nanofiber Systems Investigated

	desorption parameters					
nanofiber composition	τ_r, h	D_{eff}, cm^2/s	ρ_p[a], g/cm^3	$k(T)$, g/cm^3	E, kJ/mol	α
11% PCL+BSA[b]	14.13	1.97×10^{-13}	1.14	2.24×10^{-10}	38.19	0.87
13% PCL+BSA[b]	15.53	1.79×10^{-13}	1.14	2.04×10^{-10}	38.43	0.6
15% PCL+BSA[b]	22.24	1.25×10^{-13}	1.14	1.42×10^{-10}	39.32	0.4
11% PCL−1:0 AI:BSA[c]	4.78	5.8×10^{-13}	1.14	6.62×10^{-10}	35.48	0.33
11% PCL−1:1 AI:BSA[c]	4.57	6.08×10^{-13}	1.14	6.93×10^{-10}	35.37	0.35
11% PCL−1:10 AI:BSA[c]	4.33	6.42×10^{-13}	1.14	7.32×10^{-10}	35.24	0.53
11% PCL−1:100 AI:BSA[c]	3.44	8.08×10^{-13}	1.14	9.21×10^{-10}	34.66	0.55

[a] PCL bulk density was estimated from available data[29] and the Sigma-Aldrich MSDS database. [b] Derived from data presented in Figure 2. [c] Derived from data presented in Figure 3.

The values of τ_r and D_{eff} obtained with this estimation are presented (Table 1). The desorption factor, $k(T)$, is described by the Clapeyron-like (or the Arrhenius-like) dependence (eq 7) with the pre-exponential, k_0, having dimensionality of density (g/cm^3). The values of τ_r and D_{eff} appear to be essentially insensitive to PCL concentration, similar to the previous findings for small-molecule dye release from 11−15% PCL nanofibers. The values of the desorption enthalpy, E, are only slightly higher than the values of E = 37.3−37.8 kJ/mol found for release of low molecular weight fluorescent dye.[12] The increase of E to the level of 38.2−39.3 kJ/mol constitutes the effect of a change in the chemical nature of the released compound, as well as of an increase in its molecular weight. Although this does suggest that the desorption energy is influenced by the chemistry of the released molecule, the specific interactions are not accounted for in this theory. Overall, desorption of the fluorescent dye, rhodamine 610 chloride, from PCL nanofibers is more favored than that of BSA. However, presence and release of high molecular weight BSA macromolecules seemingly promote development of nanoporosity, which, for example, results in the higher values of the nanoporosity coefficient α for BSA (0.4−0.87) than the corresponding values of α = 0.32−0.67 for rhodamine 610 chloride.[12]

$$k(T) = k_0 \exp\left(-\frac{E}{RT}\right) \quad (7)$$

The desorption enthalpy of AI is lower than that of pure BSA (the corresponding desorption enthalpies are ∼35 kJ/mol versus greater than 38 kJ/mol, respectively) even though the molecular weight of AI (M_w = 116 kDa) is higher than that of BSA (M_w = 66 kDa). Therefore, the effect of the chemical nature of the admixture in the desorption process seems to dominate the molecular weight effect. Interestingly, the amount of BSA present in the PCL nanofibers simultaneously releasing AI and BSA has practically no effect on the value of the desorption enthalpy E (34.66−35.37 kJ/mol in the bottom three rows in Table 1). However, the value of the nanoporosity coefficient, α, differs quite significantly when BSA content in ratio to AI increases from 1 to 10, with α = 0.35 and 0.53, respectively. Therefore, the main role of BSA in such cases appears to be that of a porogen for AI. This is similar to systems reported in the literature where BSA or other proteins were released from polymer matrices.[3,4]

It should be noted that the above comparisons were made during a period of release where PCL had not begun degrading substantially and thus degradative release of the proteins can be neglected. PCL is known to have slow degradation rate in bulk objects[30] as well as in nanofibers.[31] Three-dimensional nanofibrous scaffolds composed of PCL produced by electrospinning for cartilage tissue

(29) Yang, F.; Wolkea, J. G. C.; Jansena, J. A. Biomimetic Calcium Phosphate Coating on Electrospun Poly(Epsilon-Caprolactone) Scaffolds for Bone Tissue Engineering. *Chem. Eng. J.* **2008**, *137* (1), 154–61.

engineering did not degrade appreciably in the first 21 days after immersion in the culture medium in the presence of human mesenchymal stem cells.[31] Also, PCL[32] and PCL-based[33] implants degrade *in vivo* in 2−4 years, which is significantly longer than the one month examined in this work. This was purposefully designed to allow the examination of the mechanism of release independent of the degradation of the polymeric nanofiber and the changes in release mechanisms that are present under those circumstances. The same phenomena are expected to occur in other degradable polymeric systems; however, the purely desorptive behavior would not be expected to be observable due to the significant degradation occurring in the first days of release. The desorption-limited release model would, therefore, be applicable to the release from a nondegrading systems, such as polyethylene and poly(ethylene-*co*-vinyl acetate),[4,34] more than poly(lactide-*co*-glycolide) systems.

In conclusion, the present experiments confirmed that complete release of protein contained in electrospun PCL nanofiber mats was not attained when the polymer has not degraded significantly, in agreement with the desorption-limited theory of controlled release.[12] Based upon the model presented, desorption enthalpy was affected by both chemical nature and molecular weight of the released admixture. The effect of the chemical nature of the released protein was, however, dominant. When two specific compounds, AI and BSA, were released simultaneously, BSA macromolecules facilitate release of AI, the former serving effectively as a porogen as confirmed by the increased nanoporosity factor. This theory can, therefore, be used to help understand the release of active molecules from nanofiberous materials, particularly when the material is not degrading appreciably. The theory can also be used to better design systems and properly choose formulations for incorporation into nanofibers.

Acknowledgment. This material is based upon work supported by the National Science Foundation under Grant NER-CBET 0708711. This investigation was conducted, in part, in a facility constructed with support from Research Facilities Improvement Program Grant C06 RR15482 from the National Center for Research Resources, NIH.

MP800160P

(30) Engelberg, I.; Kohn, J. Physico-Mechanical Properties of Degradable Polymers Used in Medical Applications: A Comparative Study. *Biomaterials* **1991**, *12* (3), 292–304.

(31) Li, W.-J.; Tuli, R.; Okafor, C.; Derfoul, A.; Danielson, K. G.; Hall, D. J.; Tuan, R. S. A Three-Dimensional Nanofibrous Scaffold for Cartilage Tissue Engineering Using Human Mesenchymal Stem Cells. *Biomaterials* **2005**, *26* (6), 599–609.

(32) Pitt, C. G.; Chasalow, F. I.; Hibionada, Y. M.; Klimas, D. M.; Schindler, A. Aliphatic Polyesters. I. The Degradation of Poly(Epsilon-Caprolactone) in Vivo. *J. Appl. Polym. Sci.* **1981**, *26* (11), 3779–87.

(33) Sun, H.; Mei, L.; Song, C.; Cui, X.; Wang, P. The in Vivo Degradation, Absorption and Excretion of Pcl-Based Implant. *Biomaterials* **2006**, *27* (9), 1735–40.

(34) Keskar, V.; Mohanty, P. S.; Gemeinhart, E. J.; Gemeinhart, R. A. Development of a Local System for Treatment of Cervical Cancer. *J. Controlled Release* **2006**, *115* (3), 280–8.